

Magnetocapacitance as a sensitive probe of magnetostructural changes in NiCr₂O₄Taylor D. Sparks,^{*} Moureen C. Kemei,[†] Phillip T. Barton,[‡] and Ram Seshadri[§]*Materials Department and Materials Research Laboratory, University of California, Santa Barbara, California 93106, USA*Eun-Deok Mun^{||} and Vivien S. Zapf[¶]*National High Magnetic Field Laboratory, Los Alamos National Laboratory, Los Alamos, New Mexico 87545, USA*

(Received 30 August 2013; revised manuscript received 26 November 2013; published 10 January 2014)

The spinel NiCr₂O₄ is characterized using dielectric and high-magnetic-field measurements. The trends in the magnetodielectric response fall into three clear temperature regimes corresponding to known magnetic and structural transitions. Above the Néel temperature, weak magnetic field dependence of the dielectric constant is observed with no hysteresis. Below the Néel temperature but above 30 K, a dependence of the dielectric constant on the magnetic field is observed and hysteresis develops, resulting in so-called butterfly loops. Below 30 K, magnetodielectric hysteresis is enhanced. Magnetodielectric hysteresis mirrors magnetic hysteresis, suggesting that spin-spin interactions are the mechanism for the magnetodielectric effect in NiCr₂O₄. We show that below 40 kOe, the field-dependent permittivity scales linearly with the squared magnetization as described by the Ginzburg-Landau theory. At high fields, however, the magnetization continues to increase while the dielectric constant saturates. Magnetodielectric measurements of NiCr₂O₄ suggest an additional, previously unobserved, transition at 20 K. Subtle changes in magnetism and structure at 20 K, suggest the completion of ferrimagnetic ordering and the spin-driven structural distortion. We demonstrate that magnetocapacitance is a sensitive probe of magnetostructural distortion and provide the first high-field measurements of NiCr₂O₄.

DOI: [10.1103/PhysRevB.89.024405](https://doi.org/10.1103/PhysRevB.89.024405)

PACS number(s): 75.50.Gg, 75.47.Lx, 77.22.-d

I. INTRODUCTION

Coupling of spin and charge in insulating materials can give rise to magnetodielectric effects which enable the control of magnetic polarization using an electric field or, conversely, the reversal of electric polarization by a magnetic field. However, few technologies based on the magnetodielectric effect in insulators have been realized due to the small magnitude of induced magnetic or electric polarization, weak coupling between charge and spin, and the low temperatures where magnetodielectric coupling often arises. In the past decade, intense effort has been devoted to understanding how magnetism that breaks spatial-inversion symmetry can induce ferroelectricity in so-called type-two multiferroics, especially in REMnO₃ systems.^{1,2} More recently, room-temperature magnetodielectricity due to complex spin ordering has been observed in hexaferrites.^{1,3} Electric field control of four different magnetodielectric states in the hexaferrite Ba_{0.52}Sr_{2.48}Co₂Fe₂₄O₄₁ reveals new opportunities for the next generation of memory devices based on magnetodielectric materials.⁴

Advancing the understanding of known magnetodielectric compounds is an important challenge that will guide the design of future multiferroic materials. The normal spinel NiCr₂O₄ is a known magnetodielectric that was first reported by Mufti *et al.*^{5,6} NiCr₂O₄ crystallizes in the cubic space group $Fd\bar{3}m$ above 310 K.⁵ Ni²⁺ ions have the degenerate electronic configuration $e^4 t_2^4$ in tetrahedral coordination while nondegenerate Cr³⁺ e_g^3 prefer to occupy octahedral sites. Below 310 K, orbital degeneracy on tetrahedral Ni²⁺ drives cooperative Jahn-Teller distortion of NiCr₂O₄, resulting in the lowering of average structural symmetry from cubic $Fd\bar{3}m$ to tetragonal $I4_1/amd$.^{7,8} This tetrahedral distortion results in the elongation of NiO₄ tetrahedra and $c/a > 1$. Magnetostructural coupling drives further distortion of NiCr₂O₄

from tetragonal symmetry to orthorhombic symmetry at the Néel temperature ($T_N \sim 65$ K).^{9,10} A second distortion within the orthorhombic structure takes place at $T = 30$ K, where anomalies in magnetic susceptibility and heat capacity are observed.^{8,9,11,12}

Neutron diffraction studies by Kagomiya and Tomiyasu show that the ordering of the longitudinal ferrimagnetic component of NiCr₂O₄ occurs at 60 K and this is followed by the ordering of the transverse antiferromagnetic components at 30 K.¹¹ Neutron scattering reveals four Cr³⁺ B sublattices that give rise to a net moment of $2.69 \mu_B$ along the [100] direction; this moment is compensated by the net A sublattice moment of $3.0 \mu_B$, resulting in an overall moment of $0.31 \mu_B$ per formula unit of NiCr₂O₄.¹¹ Detailed heat capacity measurements by Klemme and Miltenburg show three anomalies: at 310 K due to Jahn-Teller ordering, near 70 K, and at 29 K due to magnetostructural coupling.¹² Mufti *et al.* have reported changes in the slope of the dielectric constant of NiCr₂O₄ at 75 K and 31 K; they also show magnetic field dependence of the dielectric constant of NiCr₂O₄.⁶ Following this initial work, Maignan *et al.* measured a polarization of $13 \mu C m^{-2}$ in the ferrimagnetic state of NiCr₂O₄.¹³ Polarization in the ferrimagnetic state of the related spinels FeCr₂O₄ and CoCr₂O₄ has also been observed.¹⁴

Here we present a careful study of the temperature and magnetic field dependence of the dielectric properties of polycrystalline NiCr₂O₄, revealing three temperature regimes that describe the trends in magnetocapacitance. We provide the first high-field-magnetization measurements of the spinel NiCr₂O₄ at various temperatures. We describe the correlations between spin-spin interactions and the dielectric constant of NiCr₂O₄. We demonstrate the linear correlation between the field-dependent squared magnetization and the changes in dielectric permittivity at low fields. We also discuss the multiferroic properties of NiCr₂O₄ in the context of recent

studies of magnetostructural coupling in NiCr_2O_4 , showing that variations in magnetocapacitance occur concurrently with changes in structure and spin configuration.⁹ We illustrate the sensitivity of magnetocapacitance measurements to magnetostructural changes in NiCr_2O_4 by revealing an unreported anomaly at 20 K. Incorporating detailed magnetic and structural studies, we investigate the origin of the anomaly at 20 K. We conclude that the 20 K anomaly corresponds to the completion of structural and magnetic ordering.

II. METHODS

Phase pure powders of NiCr_2O_4 were prepared from stoichiometric amounts of NiO and Cr_2O_3 that were ground, pelletized, and annealed at 800° for 12 h. Sample pellets were reground, repelletized, and annealed at 1100° for 24 h. Structural characterization was performed using high-resolution ($\Delta Q/Q \leq 2 \times 10^{-4}$) synchrotron x-ray powder diffraction at the Advanced Photon Source, Argonne National Laboratory. Powder patterns were fit to the crystal structure using the Rietveld refinement method as implemented in the EXPGUI/GSAS program.^{15,16} Magnetic susceptibility measurements were performed using a Quantum Design (QD) Magnetic Property Measurement System. High field magnetization was measured using an extraction magnetometer in a capacitor-bank-driven 65-T pulsed-field magnet at the National High Magnetic Field Laboratory Pulsed-Field Facility at Los Alamos National Laboratory.¹⁷ Samples for magnetocapacitance measurements were spark plasma sintered at 1200 K under a load of 6 kN for 10 min with a very fast heating and cooling cycle. Spark plasma sintering was used to achieve high densities, ensuring the collection of highly reliable dielectric measurements. Densified pellets were annealed in air to 1100 K for 3 h to ensure stoichiometric NiCr_2O_4 is recovered following slight reduction during the spark plasma sintering process. Laboratory $\text{CuK}\alpha$ x-ray diffraction performed on annealed spark plasma-sintered pellets show that stoichiometric NiCr_2O_4 is obtained.

Dielectric measurements as a function of temperature and applied magnetic field were carried out using an Andeen-Hagerling AH2700A capacitance bridge connected via shielded coaxial cables to a sample located within a QD Dynacool Physical Property Measurement System. Coplanar faces of a cylindrical sample, 9.5 mm in diameter, were polished and coated with conducting epoxy to enable the connection of electrical contacts. The sample was 2.3 mm thick. Capacitance measurements were collected at several frequencies continuously as the temperature or magnetic field was varied at 3 K/min or 150 Oe/s, respectively.

III. RESULTS

Synchrotron x-ray powder diffraction of NiCr_2O_4 collected at 100 K shows that the prepared sample is well modeled by the tetragonal spacegroup $I4_1/amd$ with lattice parameters $a = 5.79183(2)$ Å and $c = 8.53835(5)$ Å. The lattice parameters reported here are in good agreement with values reported in the literature.⁹ Oxygen atoms are described by the general positions $x = 0$, $y = 0.5129(2)$, and $z = 0.2329(1)$ while

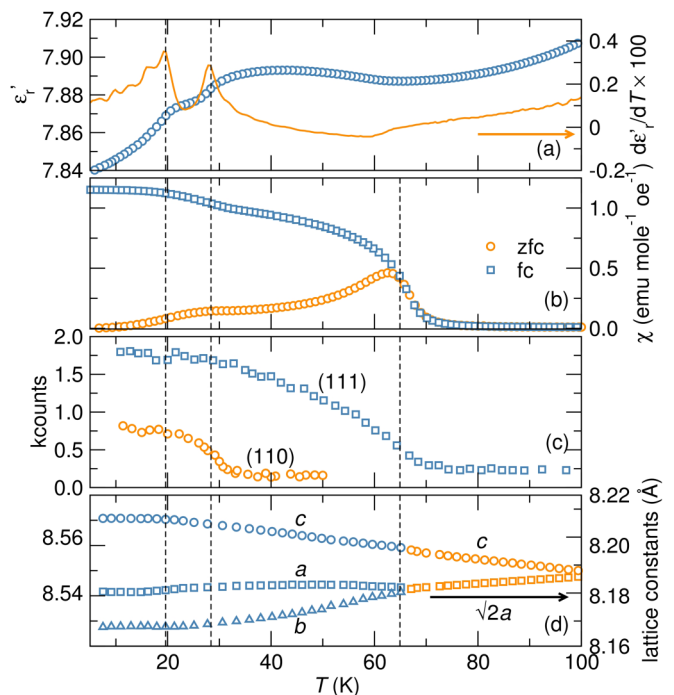


FIG. 1. (Color online) Magnetostructural and magnetodielectric coupling in NiCr_2O_4 . (a) Temperature-dependent dielectric permittivity measurements of NiCr_2O_4 collected at 20 kHz shows anomalies near 30 K and 20 K. The anomaly at 20 K has not been previously observed. The derivative of the dielectric permittivity as a function of temperature shows maxima near 20 K and 30 K. (b) Zero-field-cooled (ZFC) and field-cooled (FC) temperature-dependent magnetic susceptibility of NiCr_2O_4 reveals the onset of ferrimagnetic order at 65 K, where the ZFC and FC curves diverge. At 30 K, another change in the magnetic structure occurs. We note that below 20 K, the ZFC and FC curves saturate. Neutron diffraction studies of NiCr_2O_4 reported by Tomiyasu and Kagomiya are shown in (c).¹¹ The fundamental (111) reflection increases in intensity below 65 K while the superlattice (110) reflection increases in intensity below 30 K. The neutron reflections attain stable values below 20 K. (d) Lattice parameters of NiCr_2O_4 as a function of temperature; the tetragonal to orthorhombic transition occurs at 65 K followed by further structural change at 30 K within the orthorhombic $Fddd$ space group. Below 20 K, the lattice constants plateau.

Ni^{2+} and Cr^{3+} occupy special positions $(0, \frac{1}{4}, \frac{3}{8})$ and $(0,0,0)$, respectively.

Temperature-dependent dielectric measurements of NiCr_2O_4 show anomalies at 20 K and 30 K with clear maxima in the derivative of the dielectric permittivity as a function of temperature [Fig. 1(a)]. A shallow minimum of the temperature-dependent dielectric permittivity is observed at 65 K with no clear feature in the derivative of the dielectric permittivity with respect to temperature [Fig. 1(a)]. The temperature-dependent dielectric measurements suggests that phase transitions occur at 20 K and 30 K, where there are clear maxima in the derivative of the dielectric permittivity with respect to temperature, while magnetostriction may play a role in the slight changes in the dielectric permittivity of NiCr_2O_4 at 65 K. The dielectric permittivity anomalies correlate well with structural and magnetic transitions in NiCr_2O_4 . Ferrimagnetic ordering occurs near 65 K as shown by divergence of

zero-field-cooled and field-cooled temperature-dependent susceptibility measurements shown in Fig. 1(b). In agreement with the susceptibility studies, neutron diffraction studies by Tomiyasu and Kagomiya show the enhancement of the fundamental (111) reflections below 65 K due to the ordering of the longitudinal ferrimagnetic component of NiCr_2O_4 [Fig. 1(c)].¹¹ Further change in the magnetic structure occurs at 30 K, where another anomaly in the temperature-dependent susceptibility is observed [Fig. 1(b)] and (110) superlattice reflections emerge in neutron-scattering studies as a result of ordering of the transverse antiferromagnetic component of NiCr_2O_4 [Fig. 1(c)].¹¹ Magnetic ordering in NiCr_2O_4 is strongly coupled to structure as reported by Suchomel *et al.*⁹ At 60 K, ferrimagnetic ordering is accompanied by a tetragonal $I4_1/amd$ to orthorhombic $Fddd$ structural distortion [Fig. 1(d)]. Further change in magnetic ordering at 30 K also occurs concurrently with further structural distortion of NiCr_2O_4 within the orthorhombic $Fddd$ space group [Fig. 1(d)].

At 20 K, a clear anomaly is observed in magnetodielectric measurements of NiCr_2O_4 [Fig. 1(a)]. Reevaluation of temperature-dependent magnetic susceptibility, neutron

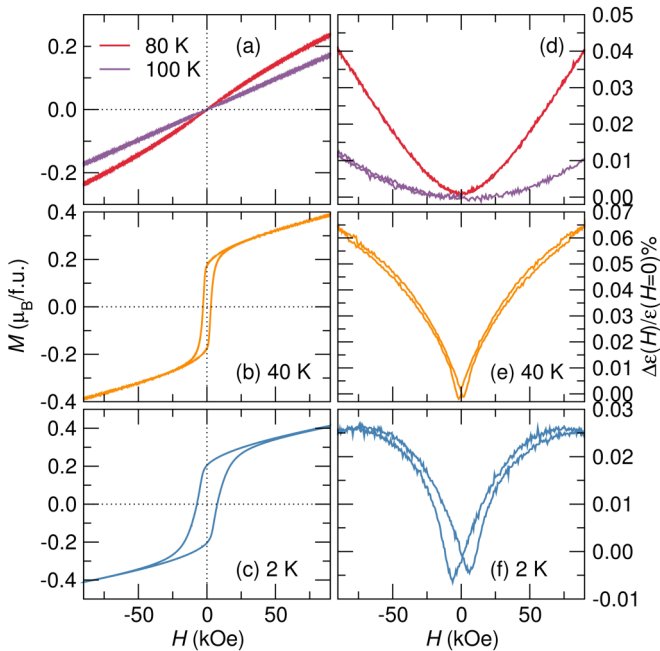


FIG. 2. (Color online) Magnetization and magnetodielectric trends in NiCr_2O_4 . Field-dependent magnetization measurements collected at (a) ≥ 80 K, (b) 40 K, and (c) 2 K are shown alongside the percentage changes in the dielectric permittivity in a varying magnetic field measured at (d) ≥ 80 K, (e) 40 K, and (f) 2 K. Above the Néel temperature, there is a weak dependence of the magnetization and the field-dependent dielectric constant on the applied field and no hysteresis [(a) and (d)]. Below the Néel temperature, slight hysteresis is observed in both field-dependent magnetization and dielectric measurements [(b) and (e)]. Below the second magnetic transition of 30 K, hysteresis is further enhanced in both magnetization and dielectric measurements. Field-dependent magnetization measurements collected at 2 K (b) and 40 K (c) show the suppression of hysteresis above 5 T.

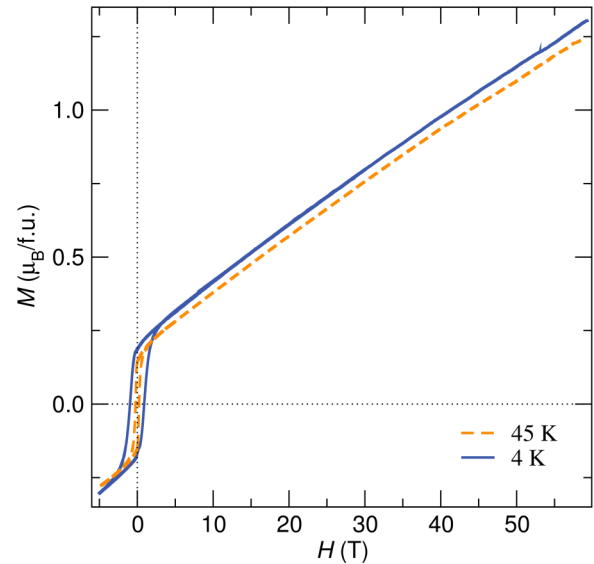


FIG. 3. (Color online) High-field-magnetization measurements of NiCr_2O_4 at 45 K and 4 K reveal a linear increase in magnetization with increase in field up to 60 T.

reflection intensities, and lattice constants reveals signatures of structural and magnetic changes at 20 K (Fig. 1). Notably, following the magnetostructural transition at 20 K, all the temperature-dependent structural and magnetic parameters attain steady values below 20 K. These trends in neutron intensity, magnetic susceptibility, and lattice parameters suggest that magnetic and structural ordering in NiCr_2O_4 occurs over a wide temperature range, between 65 K and 20 K, finally reaching completion at 20 K. This finding of the continuous change in spin and lattice structure between 65 K and 20 K is facilitated by high-precision magnetocapacitance measurements. The observation of a dielectric phase transition at 20 K that is accompanied by subtle changes in magnetism and structure of NiCr_2O_4 demonstrates that magnetocapacitance measurements are extremely sensitive to subtle magnetic and structural changes in functional materials.

There is a linear dependence of the magnetization on the applied field above the Néel temperature as shown in Fig. 2(a). Coercivity develops below the ferrimagnetic ordering temperature of NiCr_2O_4 [Fig. 2(b)]. Further enhancement of the coercivity occurs below the second magnetic ordering temperature of 30 K, as illustrated in Fig. 2(c). The highest coercivity of ~ 8.3 kOe is observed near 2 K. High-field-magnetization studies performed at 4 K and at 45 K reveal a suppression of hysteresis and a linear increase of magnetization above 2.5 T (Fig. 3). At 4 K and 60 T, the magnetization of NiCr_2O_4 is about $1.6 \mu_B$ per formula unit. This magnetization value is $2.4 \mu_B$ less than the expected value for a collinear ferrimagnetic configuration in NiCr_2O_4 , suggesting that the magnetic structure of NiCr_2O_4 reported by Kagomiya and Tomiyasu, which consists of longitudinal and transverse magnetic sublattices, persists to high fields with slight canting of spins contributing to the linear enhancement of the magnetization with field.¹¹

When ferrimagnetic interactions are present in NiCr_2O_4 , the dielectric permittivity exhibits a dependence on the applied

magnetic field. Isothermal field-dependent dielectric permittivity measurements show a parabolic dependence on the applied field near T_N . Further below T_N , a distinct dependence of the dielectric permittivity, with a sharp minimum near $H = 0$ Oe and significant increase with applied magnetic field emerges. The trends in the isothermal field-dependent dielectric measurements are well described by three temperature regimes [Figs. 2(d), 2(e), and 2(f)]. Above ~ 80 K [Fig. 2(d)], there is a very weak dependence of the dielectric permittivity on the applied field as shown by the field-dependent permittivity measured at 100 K. In the temperature range $30 \text{ K} < T < 80 \text{ K}$ [Fig. 2(e)], $\Delta\epsilon(H)/\epsilon(H=0)\%$ reaches the maximum value observed in NiCr_2O_4 of 0.065% and hysteresis develops. The dependence of the dielectric constant on the applied field when $T < 30 \text{ K}$ becomes weaker while significant hysteresis emerges in the field-dependent dielectric response [Fig. 2(f)]. As we discuss below, the trends in the three regimes follow closely the field dependence of the squared magnetization. The very subtle feature in the dielectric permittivity near 65 K suggests that magnetostriction may play a role in the observed field dependence of the dielectric permittivity in the temperature regime $30 \text{ K} < T < 80 \text{ K}$.

To ensure that the observed magnetodielectric response in NiCr_2O_4 is not merely due to magnetoresistance (Maxwell-Wagner effects), we examine the field dependence of the dissipation factor.¹⁸ Catalan has shown that magnetoresistive effects have signatures in the dielectric loss. The dissipation factor, shown in the bottom panel of Fig. 4, remains constant in a varying magnetic field while the dielectric permittivity is dependent on the applied field, indicating intrinsic magneto-capacitance in NiCr_2O_4 (Fig. 4).¹⁸

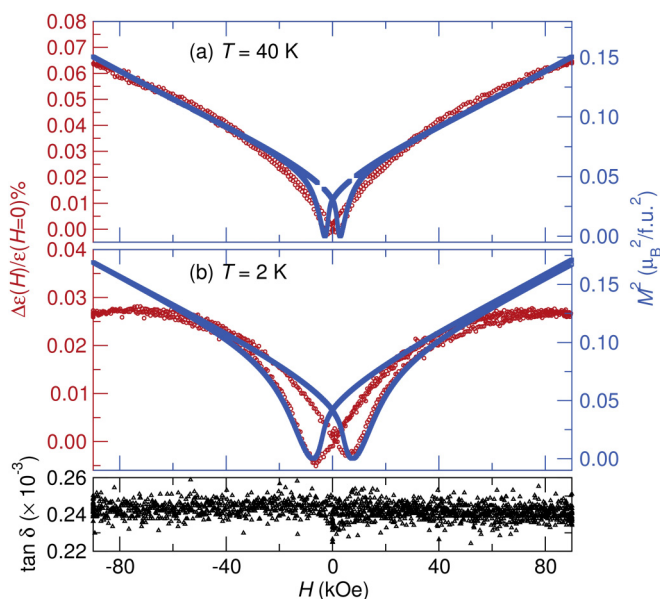


FIG. 4. (Color online) The squared field-dependent magnetization plotted against the field-dependent dielectric permittivity measurements collected at (a) 40 K and (b) 2 K. Field-dependent changes in the dielectric constant correlate with trends in the field-dependent squared magnetization at low fields. The bottom panel shows that the dissipation factor is independent of the applied field. The loss was measured at 2 K.

IV. DISCUSSION

The dielectric anomaly near 30 K occurs concurrently with changes in magnetic structure [Figs. 1(a), 1(b), and 1(c)].¹¹ This correlation supposes that magnetic perturbations couple to the dielectric constant of NiCr_2O_4 . The coupling between spin-spin correlations and phonons in NiCr_2O_4 is not surprising in light of the recent work of Suchomel *et al.* which shows lattice distortions occurring concomitantly with magnetic ordering [Fig. 1(d)].⁹ Similar spin-phonon-mediated magnetodielectric coupling has been reported for the magnetodielectrics Mn_3O_4 ,¹⁹ SeCuO_3 ,²⁰ and TeCuO_3 .²⁰

Changes in the squared magnetization in the presence of an applied field depict the trends in magnetodielectric hysteresis at low fields, as shown in Figs. 4(a) and 4(b). The relative changes in dielectric permittivity in a changing magnetic field trace the squared magnetization below 5 T (Fig. 4). Above 5 T and near 2 K, the squared magnetization continues to increase with field while the relative change in dielectric permittivity saturates [Fig. 4(b)]. The agreement between the squared magnetization and the changes in dielectric constant at low fields illustrate that the magnetodielectric coupling term $\gamma P^2 M^2$ of the Ginzburg-Landau theory for second-order phase transitions [Eq. (1)] is the most significant in NiCr_2O_4 , as was earlier proposed by Mufti *et al.*^{6,21} In the thermodynamic potential, Φ expanded to include only second-order terms as shown in Eq. (1); α , α' , and γ are temperature-dependent magnetodielectric coupling coefficients; M and P are the magnetization and polarization, respectively; and E and H are the electric and magnetic fields, respectively. The electric permittivity can be derived from the second partial derivative of the thermodynamic potential with respect to polarization, as indicated in Eq. (2). These expressions yield a linear relationship between ϵ and M^2 , as shown in Eq. (4). We find that this spin-mediated magnetodielectric coupling is most significant at low fields. Field-dependent dielectric measurements and the squared magnetization were interpolated over the field range $0 \text{ kOe} \leq H \leq 90 \text{ kOe}$. A linear relationship between $\Delta\epsilon(H)$ and $M^2(H)$ is observed when $10 \text{ kOe} \leq H \leq 50 \text{ kOe}$, as illustrated in Fig. 5. Above 50 kOe, the magnetization continues to increase with the applied field while the dielectric permittivity plateaus (Fig. 5),

$$\Phi = \Phi_0 + \alpha P^2 - PE + \alpha' M^2 - MH + \gamma P^2 M^2, \quad (1)$$

$$\frac{1}{\chi_e} = \frac{\partial^2 \Phi}{\partial P^2} = 2\alpha + 2\gamma M^2, \quad (2)$$

$$\epsilon = \chi_e + 1 = \frac{1}{2\alpha + 2\gamma M^2} + 1, \quad (3)$$

$$\epsilon \approx 1 + \frac{1}{2\alpha} \left(1 - \frac{\gamma}{\alpha} M^2 \right). \quad (4)$$

The magnetodielectric response, particularly the field dependence of capacitance, yields unique insight to subtle structural distortions in NiCr_2O_4 . The details of the structural change at 30 K in NiCr_2O_4 are not known beyond a slight change in temperature-dependent lattice constants resulting from the elongation of NiO_4 tetrahedra. Nevertheless, the

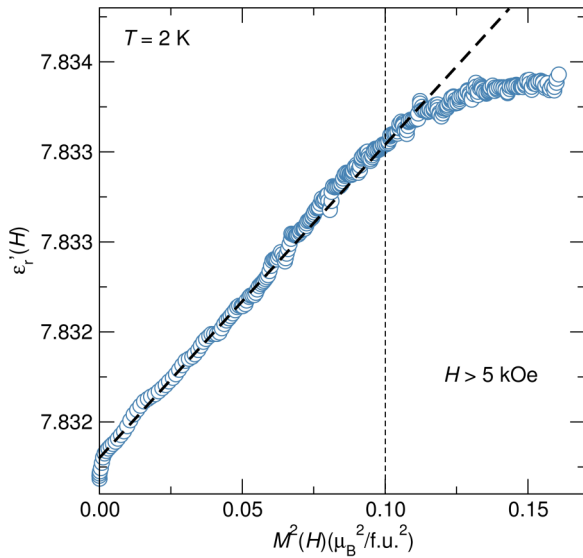


FIG. 5. (Color online) A linear relationship is observed between the measured $\epsilon(H)$ plotted against $M^2(H)$ for $10 \text{ kOe} \leq H \leq 50 \text{ kOe}$ near 2 K.

increased magnitude in magnetodielectric hysteresis could possibly suggest a cation off-centering that was not observed in previous structural studies. Polarization measurements by Maignan *et al.* have demonstrated that NiCr_2O_4 is indeed a multiferroic with polarization that develops near the Néel temperature and continues to increase until 20 K, where it approaches a steady value.¹³

V. CONCLUSION

In summary, the magnetodielectric response of dense, single-phase NiCr_2O_4 samples was measured as a function of field and temperature. The largest magnetodielectric hysteresis was observed in the *Fddd* phase below 30 K while the largest, $\Delta\epsilon(H)/\epsilon(H=0)\% = 0.06\%$, was also observed in the *Fddd* phase but in the temperature range $30 \text{ K} \leq T \leq 65 \text{ K}$. We

discuss magnetocapacitance in the context of recently reported magnetostructural coupling in NiCr_2O_4 . We demonstrate the coupling of the spin-spin correlation function to the dielectric constant of NiCr_2O_4 , which results in three temperature regimes with varying trends in magnetocapacitance. We show the linear correlation between the field-induced changes in dielectric permittivity and the squared magnetization in NiCr_2O_4 below 50 kOe. We report a 20 K anomaly in NiCr_2O_4 that is evident in magnetodielectric measurements and has subtle features in structural and magnetic order parameters. The features in temperature-dependent magnetic susceptibility and lattice parameters of NiCr_2O_4 at 20 K suggest the completion of spin and structural transformations. We show that magnetocapacitance is a sensitive probe of magnetostructural coupling in NiCr_2O_4 . We present high-field-magnetization studies of the spinel NiCr_2O_4 which show a linearly increasing magnetization up to 60 T at 45 K and 4 K.

ACKNOWLEDGMENTS

This project was supported by the NSF through the DMR 1105301. M.C.K. was supported by a Schlumberger Foundation Faculty for the Future fellowship. P.T.B. was supported by a National Science Foundation Graduate Research fellowship. We acknowledge the use of shared experimental facilities of the Materials Research Laboratory, an NSF MRSEC, supported by NSF DMR 1121053. The 11-BM beamline at the Advanced Photon Source was supported by the DOE, Office of Science, Office of Basic Energy Sciences, under Contract No. DE-AC0206CH11357. The National High Magnetic Field Laboratory was supported by the National Science Foundation through Cooperative Grant No. DMR 1157490, the State of Florida, and the US Department of Energy. We thank B. C. Melot for helpful discussions and assistance in designing and building the magnetocapacitance measurement system. M.C.K. thanks David Poerschke for assistance with the spark plasma sintering process and Bryan A. Myers for insightful discussions.

*Current address: Materials Science and Engineering Department University of Utah, Salt Lake City, UT 84112; sparks@eng.utah.edu.

†kemei@mrl.ucsb.edu

‡pbaron@mrl.ucsb.edu

§seshadri@mrl.ucsb.edu

||edmun@lanl.gov

¶vzapf@lanl.gov

¹T. Kimura, *Annu. Rev. Condens. Matter Phys.* **3**, 93 (2012).

²T. Kimura, T. Goto, H. Shintani, K. Ishizaka, T. Arima, and Y. Tokura, *Nature* **426**, 55 (2003).

³Y. Kitagawa, T. H. Y. Hiraoka, T. Ishikura, H. Nakamura, and T. Kimura, *Nat. Mater.* **9**, 797 (2010).

⁴S. W. Chun, Y. S. Chai, B.-G. Jeon, H. J. Kim, Y. S. Oh, I. Kim, H. Kim, B. J. Jeon, S. Y. Haam, J.-Y. Park *et al.*, *Phys. Rev. Lett.* **108**, 177201 (2012).

⁵O. Crottaz, F. Kubel, and H. Schmid, *J. Mater. Chem.* **7**, 143 (1997).

⁶N. Mufti, A. A. Nugroho, G. R. Blake, and T. T. M. Palstra, *J. Phys.: Condens. Matter* **22**, 075902 (2010).

⁷J. D. Dunitz and L. E. Orgel, *J. Phys. Chem. Solids* **3**, 20 (1957).

⁸V. Kocsis, S. Bordács, D. Varjas, K. Penc, A. Abouelsayed, C. A. Kuntscher, K. Ohgushi, Y. Tokura, and I. Kézsmárki, *Phys. Rev. B* **87**, 064416 (2013).

⁹M. R. Suchomel, D. P. Shoemaker, L. Ribaud, M. C. Kemei, and R. Seshadri, *Phys. Rev. B* **86**, 054406 (2012).

¹⁰H. Ishibashi and T. Yasumi, *J. Magn. Magn. Mater.* **310**, e610 (2007).

¹¹K. Tomiyasu and I. Kagomiya, *J. Phys. Soc. Jpn.* **73**, 2539 (2004).

¹²S. Klemme and J. C. van Miltenburg, *Phys. Chem. Miner.* **29**, 663 (2002).

¹³A. Maignan, C. Martin, K. Singh, C. Simon, O. I. Lebedev, and S. Turner, *J. Solid State Chem.* **195**, 41 (2012).

- ¹⁴K. Singh, A. Maignan, C. Simon, and C. Martin, *Appl. Phys. Lett.* **99**, 172903 (2011).
- ¹⁵B. Toby, *J. Appl. Crystallogr.* **34**, 210 (2001).
- ¹⁶A. C. Larson and R. B. Von Dreele, Los Alamos National Laboratory Report LAUR 86-748 (1994).
- ¹⁷J. A. Detwiler, G. M. Schmiedeshoff, N. Harrison, A. H. Lacerda, J. C. Cooley, and J. L. Smith, *Phys. Rev. B* **61**, 402 (2000).
- ¹⁸G. Catalan, *Appl. Phys. Lett.* **88**, 102902 (2006).
- ¹⁹R. Tackett, G. Lawes, B. C. Melot, M. Grossman, E. S. Toberer, and R. Seshadri, *Phys. Rev. B* **76**, 024409 (2007).
- ²⁰G. Lawes, A. P. Ramirez, C. M. Varma, and M. A. Subramanian, *Phys. Rev. Lett.* **91**, 257208 (2003).
- ²¹T. Kimura, S. Kawamoto, I. Yamada, M. Azuma, M. Takano, and Y. Tokura, *Phys. Rev. B* **67**, 180401(R) (2003).